



## Determination of $[Mg^{2+}]_i$ – an update on the use of $Mg^{2+}$ -selective electrodes

Dorothee Günzel\* & Wolf-Rüdiger Schlue

*Institut für Neurobiologie, Heinrich-Heine-Universität Düsseldorf, Universitätsstr. 1, D-40225 Düsseldorf, Germany; \*Author for correspondence (Tel: +49-211-8113418; Fax: +49-211-8113415; E-mail: guenzel@uni-duesseldorf.de)*

### Abstract

Since their invention, ion-selective microelectrodes have become an indispensable tool for investigations of intracellular ion regulation and transport. While highly selective sensors for all major intracellular monovalent ions have been available for decades, the development of sensors for divalent cations seems to have presented more difficulties. As ion-selective microelectrodes typically have time-constants in the range of 0.5 to several seconds they turned out to be inapt for the investigation of intracellular  $Ca^{2+}$ . The development of sensors for  $Mg^{2+}$ -selective electrodes has made its most striking progress only over the past few years. While the first  $Mg^{2+}$  sensor, ETH 1117, was barely able to detect physiological  $Mg^{2+}$  concentrations in the presence of other mono- and divalent cations, the newest sensors allow measurements in the micromolar range. When used in macroelectrodes, the most recent developments, ETH 5506 and ETH 5504, have even been reported to do so in the presence of millimolar  $Ca^{2+}$  concentrations. Although there is still room for improvement to make these sensors applicable in microelectrodes, some preliminary data look extremely promising and indicate that a new era for  $Mg^{2+}$ -selective microelectrodes is about to start.

### Introduction

Ion-selective microelectrodes have now been used for almost half a century, since Caldwell developed the first pH-sensitive microelectrodes in 1954. These first ion-selective microelectrodes were constructed from ion-sensitive glass initially only available for pH, but later also for  $Na^+$  and  $K^+$ . The ion-selective microelectrodes used today are mostly based on the so-called liquid membrane electrodes that were developed some 15 years later (Orme 1969,  $Ca^{2+}$ ,  $Ca^{2+}+Mg^{2+}$ ,  $Cl^-$ ; Walker 1971,  $K^+$ ,  $Cl^-$ ). Since then the number of sensors for a large variety of ion species has increased rapidly, and now includes sensors for pH,  $Na^+$ ,  $K^+$ ,  $Li^+$ ,  $Ca^{2+}$ ,  $Mg^{2+}$ ,  $Cl^-$ ,  $NO_3^-$ ,  $NH_4^+$ .

In parallel to the development of ion-selective microelectrodes another major technique for the direct measurement of intracellular free ion concentrations was introduced, namely ion-sensitive fluorescence dyes. Both techniques have various advantages and

disadvantages that render one or the other more suitable for a specific preparation or type of investigation (for rev. see also Alvarez-Leefmans *et al.* 1987):

- A major advantage of ion-selective microelectrodes over microfluorimetric measurements is the fact that the membrane potential ( $E_m$ ) is measured simultaneously, so that the condition of the preparation is constantly monitored.
- A further advantage of ion-selective microelectrodes is that electrodes, with very few exceptions, cannot penetrate intracellular organelles, so that their response exclusively reflects concentration changes within the cytoplasm. In contrast, fluorescence dyes, especially when used in their ester form, will always yield a combined signal from both the cytoplasm and the matrix of cell organelles.
- Once successfully impaled, microelectrodes allow continuous recording as long as the impalement holds which, in non-contracting preparations, may be for up to several hours. In contrast, the duration

of microfluorimetric experiments is generally limited to about one hour due to bleaching, leakage and in some cases even active extrusion of the dye from the cells.

- Fluorescence dyes used in microfluorimetric experiments may increase the intracellular buffering power of the measured ion significantly. This may decrease the intracellular free ion concentration and damp changes in these ion concentrations. Such effects can be ruled out if ion-selective microelectrodes are used.
- The greatest disadvantage of ion-selective microelectrodes is that their use is limited to relatively large, robust cells. Within these cells, ion-selective microelectrodes only monitor changes at one specific location, while microfluorimetry can be used to visualize intracellular concentration gradients when used in imaging systems.
- A further disadvantage of ion-selective microelectrodes is that due to their relatively long time constants (in the range of about one to several seconds) they are unable to record rapid transients, such as those known to occur in the intracellular free  $\text{Ca}^{2+}$  concentration.
- Both, ion-sensitive microelectrodes and fluorescence dyes are affected by a variety of interfering substances that have to be carefully evaluated in order to enable a reliable interpretation of the experimental result.

### Construction of ion-selective microelectrode

The basic electrochemistry of ion-sensitive microelectrodes, their advantages and disadvantages for use in physiological experiments and various ways to manufacture these electrodes have been described in great detail (see, e.g., Amman 1986; Thomas 1978). In brief, these electrodes consist of a glass capillary that is pulled out to form a small tip (diameter typically  $< 1 \mu\text{m}$ ). The tip of the electrode is filled with a liquid membrane consisting of an organic phase (e.g., 2-nitrophenyl octyl ether), containing an additive (e.g., potassium tetrakis(4-chlorophenyl)borate) to reduce the electrical resistance, and an ionophore that is specific for a certain ion species. The shaft of the electrode is filled with an electrolyte (backfill solution) that should contain the measured ion species and  $\text{Cl}^-$  to yield a stable potential at the chlorided silver wire that is inserted into the shaft of the electrode and through which the electrode is connected to the ampli-

fier. When an ion-selective microelectrode is impaled into a cell, the electrode records the membrane potential ( $E_m$ ) of this cell plus the ionic potential ( $E_{\text{ion}}$ ) due to the gradient of the measured ion across the liquid membrane. In order to measure  $E_{\text{ion}}$  it is necessary to determine  $E_m$  with a separate intracellular reference electrode and then to subtract  $E_m$  from the output signal of the ion-selective electrode. As conditions within the shaft of the electrode can be considered constant,  $E_{\text{ion}}$  depends on the ion concentration at the tip of the electrode.

Crucial for stabilising the hydrophobic membrane phase in the tip of the ion-selective microelectrode and thus for obtaining functional electrodes is a proper silanization of the glass capillary prior to filling. Generally, silanization involves the exposure of the glass capillaries to the vapour of a methylsilyl compound such as hexamethyldisilazan or dimethyltrimethylsilylamine and a subsequent baking of the capillaries at temperatures  $\geq 200^\circ\text{C}$  (Ammann 1986, Munoz *et al.* 1983, Tsien & Rink 1980; Thomas 1978). This is relatively straightforward if conventional, single-barrelled glass capillaries are being used. More sophisticated methods are required if the ion-selective electrodes are to be combined with a reference electrode to form double- or even multi-barrelled microelectrodes as described below (Borrelli *et al.* 1985; Rönna 1984, Coles & Tsacopoulos 1977).

The simplest method for filling liquid membrane microelectrodes is the front filling method. Here the electrolyte chosen as backfill solution is filled into the silanized capillary and forced into the tip by using pressure. The tip of the capillary is then immersed into the liquid membrane, which is drawn into the tip either spontaneously by capillary force or by applying suction. The great advantage of this method is that it generates very short liquid membrane columns, typically between 50 and 200  $\mu\text{m}$ , which minimize the electrical resistance of the electrode. The major disadvantage is that this method requires relatively large tip diameters or very high pressures as decreasing tip sizes make it increasingly difficult to force the electrolyte into the silanized and therefore hydrophobic capillary.

For the alternative back-filling technique the liquid membrane is filled into the capillary from the shaft, i.e. the back end of the capillary, before it is overlaid by the backfill solution. In these electrodes the height of the liquid membrane column may exceed 1 cm. Major difficulties during the filling procedure are the formation of air-bubbles within the membrane column

(these may be removed by storing the electrodes in a vacuum for some time before adding the backfill solution) and at the interface between the membrane column and the backfill solution. This method is much more time consuming than the front-filling technique; however, it allows the use of considerably smaller tip diameters and the construction of double- and even multi-barrelled electrodes for the simultaneous measurement of several ion species.

The use of double-barrelled microelectrodes is a convenient way of combining the ion-selective microelectrode with the intracellular reference electrode, thus preventing the need to impale a single cell with two separate electrodes. This is especially advantageous if the cells are either small or if they may contract, shrink or swell during the experimental procedure. In electrically active cells double-barrelled microelectrodes also ensure that the intracellular reference potential is determined in the same spot as the potential of the ion-sensitive microelectrode.

Double-barrelled microelectrodes either consist of two glass capillaries glued together or a so-called theta-type capillary that contains a partitioning wall so that the cross-section of such a capillary looks like the Greek letter  $\theta$ . Pulling out such capillaries results in a single tip with two openings. One side of such a double-barrelled capillary has to be silanized before being filled as described above, to be used as the ion-selective electrode. The other side needs to be prevented from being silanized so that it can be filled with an electrolyte solution such as 3 M KCl to be used as intracellular reference electrode. This selective silanization can be achieved, e.g., by continuous perfusion of the future reference channel with compressed air. By combining a single-barrelled and a theta-style capillary or even two theta-style capillaries the same technique can be used to construct three- and four-barrelled microelectrodes (Günzel *et al.* 1997, 1999).

### Calibration of ion-selective microelectrodes

Each ion-selective microelectrode should be calibrated before and after every experiment. There are numerous ways for calibrating ion-selective microelectrodes (for rev. see Ammann 1986; W. Zhang *et al.* 1998; Thomas 1978). Personally, we favour using calibration solutions with a fixed ionic background to mimic intracellular conditions and thereby to minimize effects of interfering ions ('unorthodox' calibration, Thomas

1978). As all microelectrodes, possibly with the exception of pH-electrodes, do not show ideal Nernstian behaviour in the physiologically relevant range, more than two, usually four to seven, calibration solutions have to be used. The obtained calibration data can then be fitted with the Nicolsky-Eisenman equation (see Figure 1, for a detailed description of the equation see Ammann, 1986 and W. Zhang *et al.* 1998), which, in its simplified form can be written as:

$$E_{\text{ion}} = C + s_{\text{max}} \cdot \log(a + a_0) \quad (1)$$

with  $E_{\text{ion}}$ , ionic potential;  $C$ , constant;  $s_{\text{max}}$ , maximum (Nernstian) slope ( $s = \ln(10)RT/zF$ , where  $R$ ,  $T$ ,  $F$  and  $z$ , have their usual meaning)  $a$ , activity of the measured ion,  $a_0$ , detection limit of the electrode expressed as ion activity.

Both, the Nernst equation and the Nicolsky-Eisenman equation require the use of ion activities, not concentrations. To convert the ion concentrations of the calibration solutions into activities, the activity coefficient of a given calibration solution can be calculated using the Debye-Hückel formalism (see Ammann 1986). During intracellular recordings, the output voltage of an electrode can then be converted into an ion activity, using the determined calibration curve. As the composition of the cytoplasm is usually not sufficiently well known, this intracellular activity value cannot be converted back into a concentration. If the activity coefficient of the measured ion within the calibration solutions cannot be calculated, the most accurate way would be to describe the measured values as having the same activity as a calibration solution with a certain concentration (see Alvarez-Leefmans *et al.* 1984, 1986).

Usually, however, it is simply assumed that the ionic strength and therefore the activity coefficient of the measured ion in the cytoplasm is similar to that of the calibration solutions and the intracellular value is then given as a concentration. The Nicolsky-Eisenman equation is therefore written as:

$$E_{\text{ion}} = C + s_{\text{max}} \cdot \log(c + c_0) \quad (2)$$

$c$ , concentration of the measured ion;  $c_0$ , detection limit of the electrode expressed as concentration

Although not strictly correct, the error introduced by this assumption is probably well within the range of the general accuracy of the method. Giving values as concentrations also has the advantage that values obtained by various other methods can be compared much more directly to those obtained with ion-selective microelectrodes.

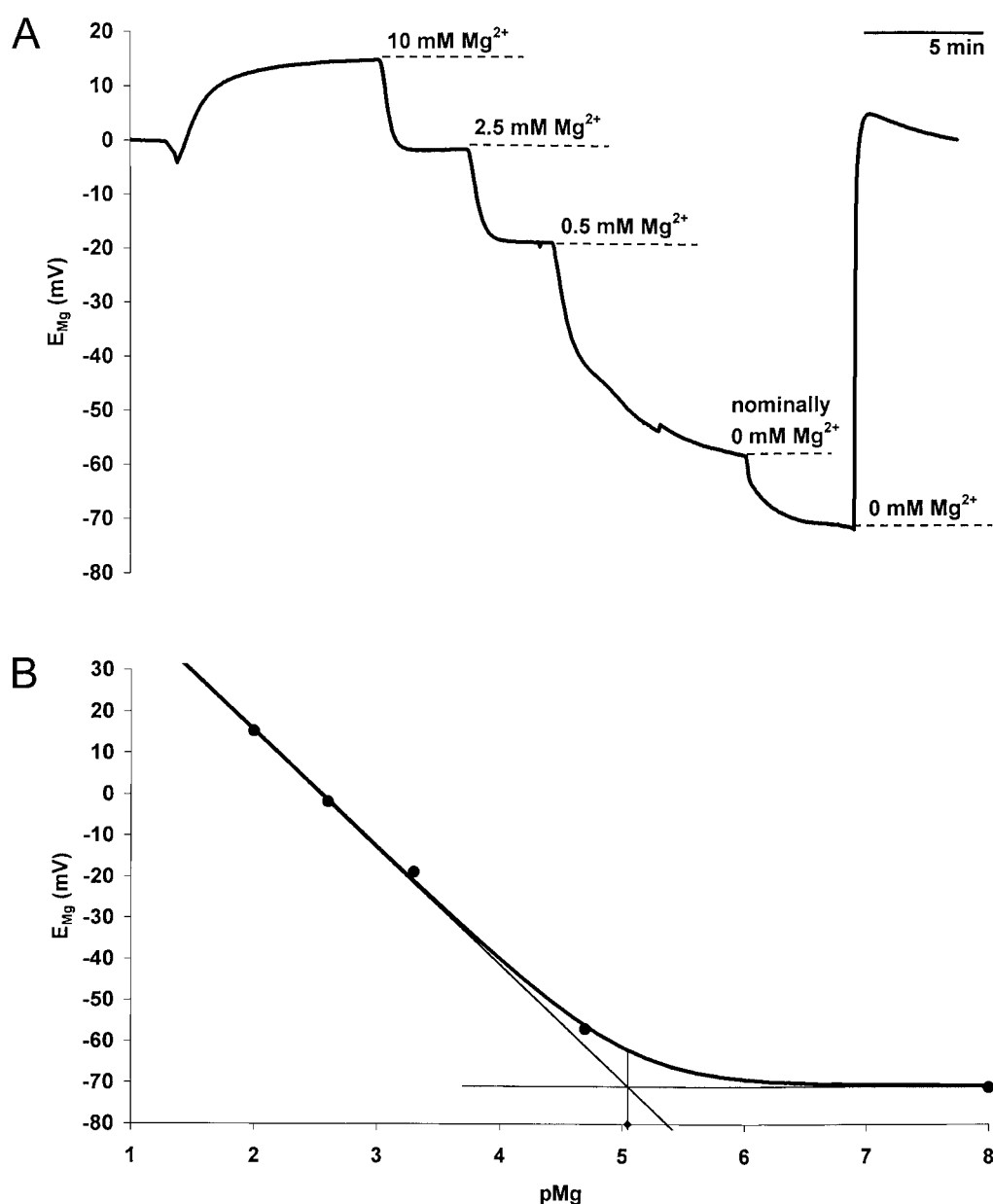


**Figure 1.** Calibration of a  $Mg^{2+}$ -selective microelectrode based on the sensor ETH 5504. (A) Recording of the potential output,  $E_{Mg}$ , of the electrode during the calibration procedure. The calibration solutions contained an ionic background of 80 mM KCl, 10 mM NaCl, 10 mM HEPES, pH adjusted to 7.3 with KOH.  $Mg^{2+}$  was added from a 1 M  $MgCl_2$  stock solution (FLUKA) to a final concentration of 10 mM, 2.5 mM and 0.5 mM, respectively. The nominally  $Mg^{2+}$  free calibration solution contained approximately  $20 \mu M Mg^{2+}$ . In the '0 mM  $Mg^{2+}$ ' solution the residual  $Mg^{2+}$  was buffered with 3 mM EDTA. The free  $Mg^{2+}$  concentration in this solution was assumed to be below  $10^{-8}$  M. (B) Plot of the  $E_{Mg}$  values obtained from the calibration shown in A against the  $pMg$  values of the calibration solutions (●). The values are fitted with the Nicolsky-Eisenman equation (thick line) assuming a  $s_{max}$  of  $-28.2$  mV/decade and a detection limit of  $9.0 \mu M$ . Thin lines depict the asymptotes of the fitted curve. The projection of the intercept of the asymptotes onto the x-axis yields the detection limit ( $pMg$  5.05) of the electrode.

As shown in Figure 1, the shape of a calibration curve, as derived from the Nicolsky-Eisenman equation can be described by two parameters: the maximum (Nernstian) slope,  $s_{\max}$ , at high ion concentrations and the detection limit,  $c_0$ , defined as the ion concentration at the intercept of the two asymptotes of the curve (Ammann 1986). By adjusting the numerical value of  $C$ , the values obtained during an electrode calibration can be fitted with the Nicolsky-Eisenman equation. In theory, it is therefore sufficient to calibrate an ion-selective microelectrode in three calibration solutions: two solutions containing high concentrations of the measured ion to determine  $s_{\max}$  and one solution not containing the measured ion, to be able to determine  $c_0$ . It is, however, advisable to add at least one calibration solution with a concentration close to the expected intracellular concentration of the measured ion. The three values determined during calibration,  $s_{\max}$ ,  $c_0$  and  $C$  are sufficient to calculate the free ion concentration,  $c$ , at any time during a recording by solving the Nicolsky-Eisenman equation for the ion concentration  $c$ :

$$c = 10^{(E_{\text{ion}} - C)/s_{\max}} - c_0. \quad (3)$$

Relevant for the resolution and thus for the accuracy of a measured value is the slope within the physiological concentration range of this ion,  $s_{\text{physiol}}$ , which can be calculated as:

$$s_{\text{physiol}} = s_{\max} \cdot \frac{c}{c + c_0} \quad (4)$$

Thus, the resolution of ion-selective microelectrodes is generally better for monovalent ions than for divalent ions and increases with increasing  $c/c_0$ . As can be seen from this equation,  $s_{\text{physiol}}$  will only be 50% of  $s_{\max}$  if  $c$  equals  $c_0$ . Assuming that for optimal performance  $s_{\text{physiol}}$  should be at least 90%  $s_{\max}$  this means that the detection limit of an ion-selective microelectrode should be less than 1/9 of the expected intracellular ion concentration.

According to the Nicolsky-Eisenman equation,  $c_0$  should only depend on the concentrations of the interfering ions and their respective selectivity coefficients. It has been found, however, that other factors such as tip diameter and membrane resistance also influence  $c_0$  (Spichiger & Fakler 1997). Therefore, the performance especially of very fine electrodes may be considerably less than expected from the given selectivity coefficients. In some cases, the quality of ion-selective microelectrodes may be greatly improved by bevelling the electrode tip.

Finally, as pointed out by Fry *et al.* (1990) it has to be kept in mind that the recorded potential is proportional to the logarithm of the ion concentration (or the  $\text{pIon} = -\log [\text{Ion}]$ ) but not to the ion concentration itself. Thus, if the potentials recorded e.g. during a determination of the intracellular resting levels for a certain ion species show a normal distribution, the  $\text{pIon}$  values are also normally distributed (at least if  $[\text{Ion}]$  is far above  $c_0$ , or if the scatter of the values is small) but not the values of the free intracellular ion concentration,  $[\text{Ion}]_i$ . Averaging individual  $[\text{Ion}]_i$  values therefore overestimates the mean  $[\text{Ion}]_i$  value. To obtain a more accurate estimate of the mean  $[\text{Ion}]_i$  the individual  $\text{pIon}$  values should be averaged and the resulting mean  $\text{pIon}$  value can then be converted into a mean  $[\text{Ion}]_i$ .

## Mg<sup>2+</sup>-selective microelectrodes

### ETH 1117

The first Mg<sup>2+</sup>-ionophore used for measuring the intracellular free Mg<sup>2+</sup> concentration ( $[\text{Mg}^{2+}]_i$ ) was developed about 20 years ago (ETH 1117, Lanter *et al.* 1980). However, the use of this sensor for intracellular Mg<sup>2+</sup> determinations was very limited, not, in spite of wide-spread prejudice, because of the lack of selectivity for Mg<sup>2+</sup> over Ca<sup>2+</sup> but because of the lack of selectivity for Mg<sup>2+</sup> over K<sup>+</sup>. In solutions simulating intracellular conditions (100 mM K<sup>+</sup>, 10 mM Na<sup>+</sup>, 10<sup>-7</sup> M Ca<sup>2+</sup>) Lanter *et al.* (1980) report a detection limit of these electrodes, given as Mg<sup>2+</sup> activity, of 0.32 mM which is equivalent to a Mg<sup>2+</sup> concentration of about 0.8 mM (activity coefficient 0.38 for a ionic strength of 0.1 M, Debye-Hückel formalism, see Ammann 1986). This corresponds well to the mean detection limit estimated from calibrations given by Alvarez-Leefmans *et al.* (1984, 1986), McDermott (1990), McGuigan & Blatter (1989), Lopez *et al.* (1984) and Hess *et al.* (1982), of  $0.98 \pm 0.55$  mM (range 0.5 to 2 mM) which is at or even above the actual intracellular values (Figure 2A). According to the definition of the detection limit this means that the slope of the electrodes in this range is only half the ideal Nernstian value, i.e., less than 15 mV/pMg-unit. As Alvarez-Leefmans *et al.* (1986) showed that a 20% change in K<sup>+</sup> altered the electrode potential in the relevant range by about 3 mV this would alter the determined  $[\text{Mg}^{2+}]_i$  considerably. It is therefore not surprising that some  $[\text{Mg}^{2+}]_i$  values determined with

these electrodes were probably considerably overestimated (Lanter *et al.* 1980; Hess *et al.* 1982; Lopez *et al.* 1984, for rev. see Blatter and McGuigan 1988). Reliable determinations of  $[Mg^{2+}]_i$  could only be carried out if  $[K^+]_i$  was either known from previous studies and very stable (McGuigan *et al.* 1990) or if it was measured simultaneously and the contribution of  $K^+$  interference was taken into consideration (Alvarez-Leefmanns 1986).

#### ETH 5214

The considerably improved  $Mg^{2+}$ -ionophore ETH 5214 was developed in 1989 (Hu *et al.* 1989), immediately replaced ETH 1117 and is still in use. As ETH 1117, ETH 5214 is pH-independent and shows negligible  $Ca^{2+}$ -interference under intracellular conditions, i.e. for  $Ca^{2+}$  concentrations  $\leq 10^{-6}$  M (McGuigan *et al.* 1990; Günzel & Galler 1991), but it is unsuitable for extracellular  $Mg^{2+}$ -determinations, i.e., in the presence of millimolar  $Ca^{2+}$  concentrations. Interference through  $Na^+$  and  $K^+$  is improved; however, it still has to be taken into consideration when designing calibration solutions. Selectivity coefficients for  $Na^+$  and  $K^+$  are almost identical which implies that even large intracellular changes in  $[Na^+]_i$  and  $[K^+]_i$  are no problem as long as the sum of  $[Na^+]_i + [K^+]_i$  is roughly constant. Calculated from the selectivity coefficients given by Hu *et al.* (1989), the detection limit for electrodes based on ETH 5214 in calibration solutions containing 80 mM KCl, 10 mM NaCl and about  $10^{-6}$  M  $Ca^{2+}$  should be at a  $Mg^{2+}$  concentration of about 0.09 mM (0.03 mM Mg activity). This is in good agreement with the mean detection limit of  $0.07 \pm 0.04$  mM ( $n = 25$ ) determined by Günzel *et al.* (1997). It is sufficiently low for most preparations and experimental conditions, however, it is by no means ideal, as  $s_{physiol}$  is well below 90%  $s_{max}$  (Figure 2A).

Although microelectrodes based on the sensor ETH 5214 are well suited to measure resting levels of  $[Mg^{2+}]_i$  there are several limitations when investigating  $[Mg^{2+}]_i$  regulation. The greatest problem is that these electrodes tend to lose selectivity during longer-lasting experiments, so that in many cases a calibration carried out after an experiment differs considerably from the initial calibration. The reason for this is unclear; only part of this seems to be due to a clogging of the electrode by cell fragments that can be removed by quick rinsing under tap water. A further observation in our laboratory was an interaction of  $Mg^{2+}$ -selective microelectrodes

with unknown compounds (possibly plasticizers) from silicone-containing products such as sylgard or silicone tubing. We observed that  $Mg^{2+}$ -selective microelectrodes invariably failed to work in experimental chambers that had been freshly coated with sylgard, while other types of electrodes ( $pH$ ,  $Na^+$ ,  $K^+$ ,  $Cl^-$ ) were not affected. The resulting loss in sensitivity could be prevented if the chambers were stored in ethanol for about a week prior to use. Silicon tubing was initially used in one of the perfusion systems. If calibration solutions were left in contact with this tubing for longer periods of time,  $Mg^{2+}$ -electrodes showed a transient response that was not present if the duration of contact between the tubing and the solutions was minimized (Petra Schulte, Universität Düsseldorf, unpublished results). Similar effects of silicone on  $Mg^{2+}$ -macroelectrodes have been described by Marsoner *et al.* (1994).

The unaccounted loss of selectivity during an experiment is a serious problem for the evaluation of the data. Resting  $[Mg^{2+}]_i$  levels should only be evaluated from measurements that obey strict criteria. Various criteria have been set by different authors such as a difference of 1 mV or less between the two calibration curves obtained before and after an experiment (Blatter & McGuigan 1986; McDermott 1990; Günzel & Galler 1991) or a difference of less than 0.4 mM for the  $[Mg^{2+}]_i$  values calculated from the two calibration curves (Buri & McGuigan 1990, Hintz *et al.* 1999).

Even if a recording does not comply with these criteria, however, they may still be used for the evaluation of rates of  $Mg^{2+}$  influx or extrusion, as long as the values are not expressed as a change in  $[Mg^{2+}]_i$  per time unit but as a change in pMg per time unit. This is demonstrated in Figure 3A. In the majority of cases, calculation of pMg from the two calibration curves obtained before and after an experiment causes a parallel shift in the calculated values. Rates of changes in pMg thus remain virtually independent of the calibration used. If these values were converted into  $[Mg^{2+}]_i$  before an evaluation of the rates of de- or increase, the values calculated from the two calibrations would differ greatly (see Figure 3B).

$Mg^{2+}$ -selective microelectrodes based on ETH 5214 show strong interference through substances, such as  $Li^+$ , TMA or choline, that may be used to replace  $Na^+$  when studying the function of  $Na^+/Mg^{2+}$  antiport (Gasser 1990, McGuigan *et al.* 1993). Moreover, all drugs that are commonly used to inhibit  $Na^+/Mg^{2+}$  antiport, such as amiloride, imipramine and quinidine show severe interference (Günzel &

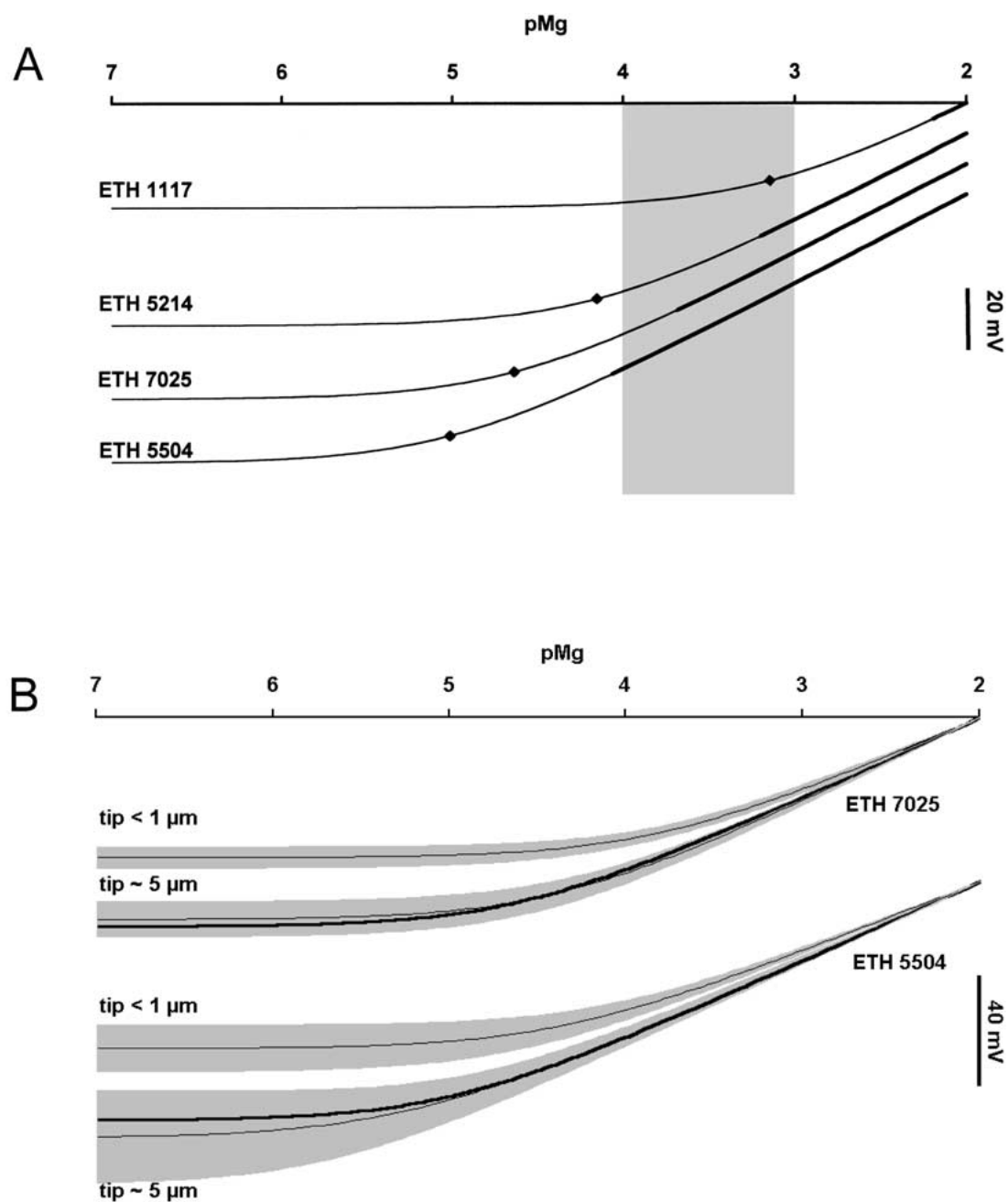


**Figure 2.** Properties of Mg<sup>2+</sup>-selective microelectrodes based on the Mg<sup>2+</sup>-sensors ETH 1117, ETH 5214, ETH 7025 and ETH 5504. (A) Theoretical relationships between pMg and the electrode potential for the four Mg<sup>2+</sup> sensors, ETH 1117, ETH 5214, ETH 7025, and ETH 5504, calculated from the published selectivity coefficients (Lanter *et al.* 1980, Hu *et al.* 1989; Schaller *et al.* 1993; Zhang *et al.* 1998, thin lines). Thick lines,  $s \geq 90\% s_{\max}$ ; ♦, detection limit; shaded area, physiological range of [Mg<sup>2+</sup>]<sub>i</sub> (B) Theoretical relationships (thick lines) and mean measured relationships (thin lines)  $\pm$  SD (shaded areas,  $n = 3-4$ ) between pMg and the electrode potential for microelectrodes based on the Mg<sup>2+</sup> sensors ETH 7025 and ETH 5504. For both sensors, microelectrodes with tips broken to a diameter of about 5  $\mu\text{m}$  had the predicted properties, while the sensitivity was considerably reduced if the tip size was < 1  $\mu\text{m}$ .

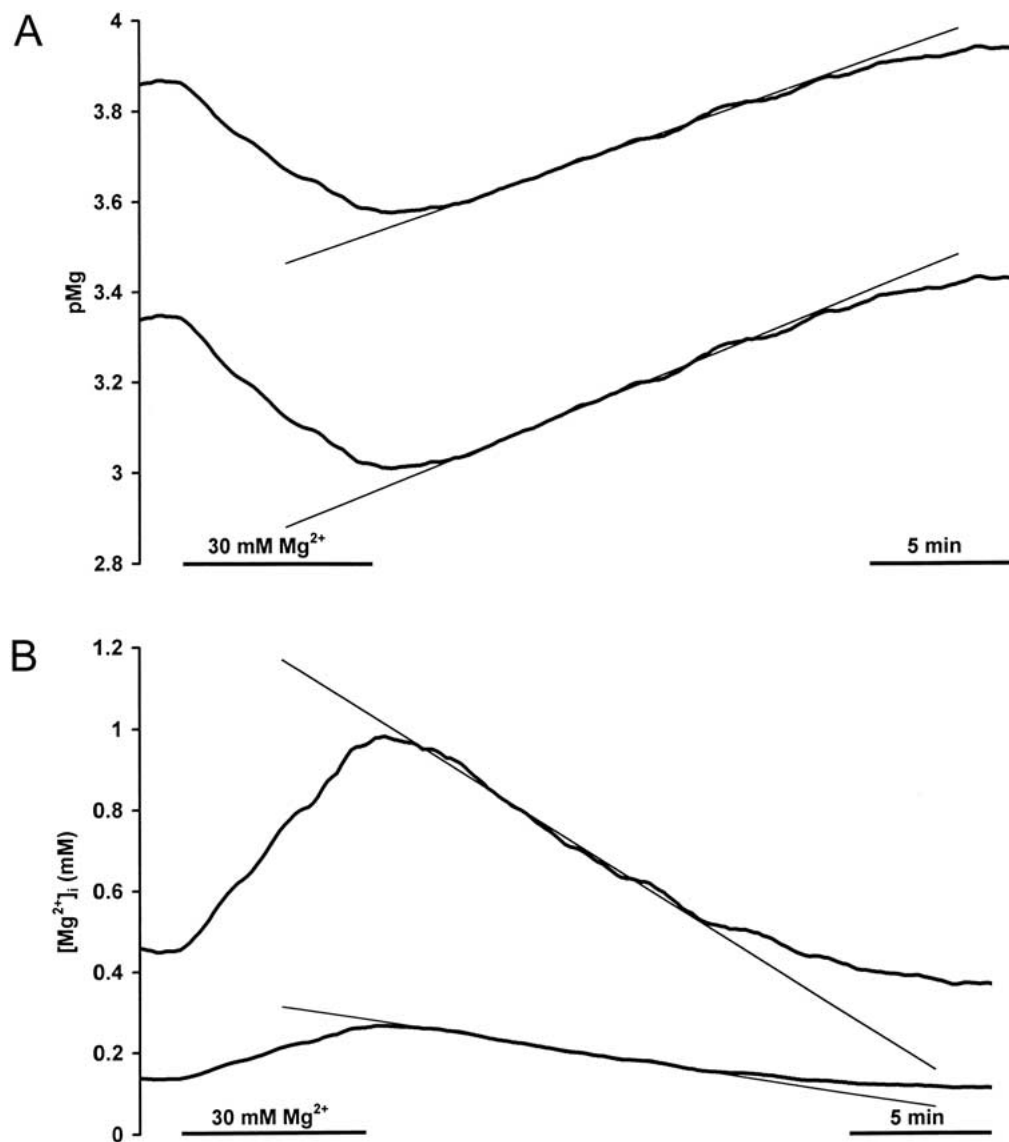


Figure 3. Recording of  $[Mg^{2+}]_i$  in a leech Retzius neurone during which the  $Mg^{2+}$ -selective microelectrode (based on ETH 5214) showed a pronounced loss in sensitivity. During a recording of  $[Mg^{2+}]_i$  in a leech Retzius neurone the cell was loaded with  $Mg^{2+}$  by increasing the extracellular  $Mg^{2+}$  concentration from 1 to 30 mM. After reducing the extracellular  $Mg^{2+}$  concentration back to 1 mM,  $Mg^{2+}$  was extruded from the neurone until  $[Mg^{2+}]_i$  reached its original value. In this experiment the calibration curves of the  $Mg^{2+}$ -selective microelectrode obtained before and after the experiment, differed greatly. The loss in sensitivity resulted in a parallel shift of the  $pMg$  values calculated from the calibration before (upper curve) and after (lower curve) the experiment. While it is impossible to determine  $[Mg^{2+}]_i$  from such an experiment, the rate of change, expressed as  $pMg/min$ , differs only marginally, as indicated by the linear regression (thin line) during the phase of  $Mg^{2+}$  extrusion. (B) If the  $pMg$ -values from A are converted into  $[Mg^{2+}]_i$  the rates of  $Mg^{2+}$  extrusion, expressed as  $(mM/min)$ , differ drastically.



Schlue 1996). In some cases, these substances may still be used, as they do not sufficiently enter the cells to elicit an electrode response. As the permeability for these drugs may depend on the cell type (Hintz *et al.* 1999), interference tests have to be carried out for each drug and preparation.

While ETH 5214 is insensitive to pH changes even over a range that by far exceeds physiological values, it does respond to  $\text{NH}_4^+$ , which is often used to induce changes in  $\text{pH}_i$  (Günzel *et al.* 1997; McGuigan *et al.* 1993).

In spite of all these difficulties related to the use of microelectrodes based on ETH 5214, these electrodes still seem to provide more reliable results than the fluorescence dyes magfura-2 and magfura-5. While magfura-5 shows strong interference from changes in  $\text{pH}_i$  (Buri *et al.* 1993), major interference at magfura-2 occurs through  $\text{Ca}^{2+}$ , even at physiological levels. This has most impressively been demonstrated by an experiment carried out by Kennedy (1998), during which she simultaneously measured  $[\text{Mg}^{2+}]_i$  with magfura-2 and a  $\text{Mg}^{2+}$ -selective microelectrode. This experiment shows that under conditions that increase  $[\text{Ca}^{2+}]_i$  the fluorescence signal shows an apparent increase in  $[\text{Mg}^{2+}]_i$  which is not at all visible in the recording of the  $\text{Mg}^{2+}$ -selective microelectrode. It thus has to be concluded that the apparent increase in  $[\text{Mg}^{2+}]_i$  indicated by the fluorescence signal was solely due to an increase in  $[\text{Ca}^{2+}]_i$ .

Discrepancies between measurements using  $\text{Mg}^{2+}$ -selective microelectrodes and magfura-2 were also found by Munsch *et al.* (1995) in leech glial cells, although here the reason for these discrepancies remained unclear.

In a study on pancreas acinar cells, both magfura-2 and  $\text{Mg}^{2+}$ -selective microelectrodes were employed to rule out contributions of changes in the free  $\text{Ca}^{2+}$  concentration in the cytoplasm and in intracellular stores to the  $\text{Mg}^{2+}$  signal. It was observed that the magfura-2 signal only paralleled the signals obtained with microelectrodes if the cells were concomitantly loaded with the  $\text{Ca}^{2+}$  buffer, BAPTA-AM (Mooren *et al.*, 2001), suggesting that increases in  $[\text{Ca}^{2+}]_i$  interfered with the signal of magfura-2 but not with that of the  $\text{Mg}^{2+}$ -selective microelectrodes.

One of the major advantages of  $\text{Mg}^{2+}$ -selective microelectrodes over other techniques for measuring  $[\text{Mg}^{2+}]_i$  is that they can easily be combined with other electrophysiological techniques, such as two-electrode voltage-clamp or iontophoretic injection of various substances. It is also possible to form multi-barrelled

microelectrodes that allow to measure the  $E_m$  and up to three different ion-species.

Triple-barrelled  $\text{Mg}^{2+}$ - and  $\text{Na}^+$ -selective microelectrodes proved to be extremely useful for investigations of  $\text{Na}^+/\text{Mg}^{2+}$ -antiport systems in neurones and glial cells of the central nervous system of the leech *Hirudo medicinalis* (Günzel & Schlue 1996; Hintz *et al.* 1999). These electrodes allow simultaneous measurement of all three parameters that determine the driving force of such an antiport,  $E_m$ ,  $[\text{Mg}^{2+}]_i$  and  $[\text{Na}^+]_i$ . Based on such recordings it is possible to make predictions about the stoichiometry of this antiport. The validity of these predictions could then be verified in experiments that combined the use of  $\text{Mg}^{2+}$ -selective microelectrodes with a two-electrode voltage-clamp (Müller *et al.* 1997a). In these experiments, the reference channel of the double-barrelled  $\text{Mg}^{2+}$ -selective microelectrode served as voltage-electrode in the voltage-clamp array, while a separate, conventional microelectrode was used for current-injection. The results of these experiments showed that the rate of  $\text{Mg}^{2+}$  extrusion from leech Retzius neurones decreased with more negative  $E_m$  values and thus supported the hypothesis, that the  $\text{Na}^+/\text{Mg}^{2+}$ -antiport in these neurones works with a stoichiometry of 1 : 1. Similarly, Kennedy (1998) voltage-clamped neurones of the snail *Helix aspersa* to  $-60$  mV while investigating  $\text{Mg}^{2+}$  extrusion, thus avoiding secondary effects resulting from depolarizations elicited by the various experimental conditions.

A relatively recent development is the construction of multi-barrelled  $\text{Mg}^{2+}/\text{Na}^+/\text{H}^+$ -sensitive microelectrodes that have been successfully used in leech neurones to determine the pH-dependence of intracellular  $\text{Mg}^{2+}$ -buffering and  $\text{Mg}^{2+}$ -sequestration (Günzel *et al.* 1997, 1999, 2001; for rev. see Günzel & Schlue 2000) and to investigate changes in  $[\text{Mg}^{2+}]_i$  induced by the activation of glutamate receptors (Müller *et al.* 1997b). Although, admittedly, such electrodes are somewhat tedious to manufacture, they proved to be essential to detect correlations between changes in intracellular ion concentrations if these changes were small and/or variable.

In the above-mentioned studies on intracellular  $\text{Mg}^{2+}$ -buffering, triple-barrelled  $\text{Mg}^{2+}/\text{H}^+$ -electrodes were also employed in control experiments in cell-sized electrolyte droplets (Günzel *et al.* 1999, 2001), demonstrating that these electrodes are not only useful in cellular but also in technical systems. In both the experiments on cells and on electrolyte droplets

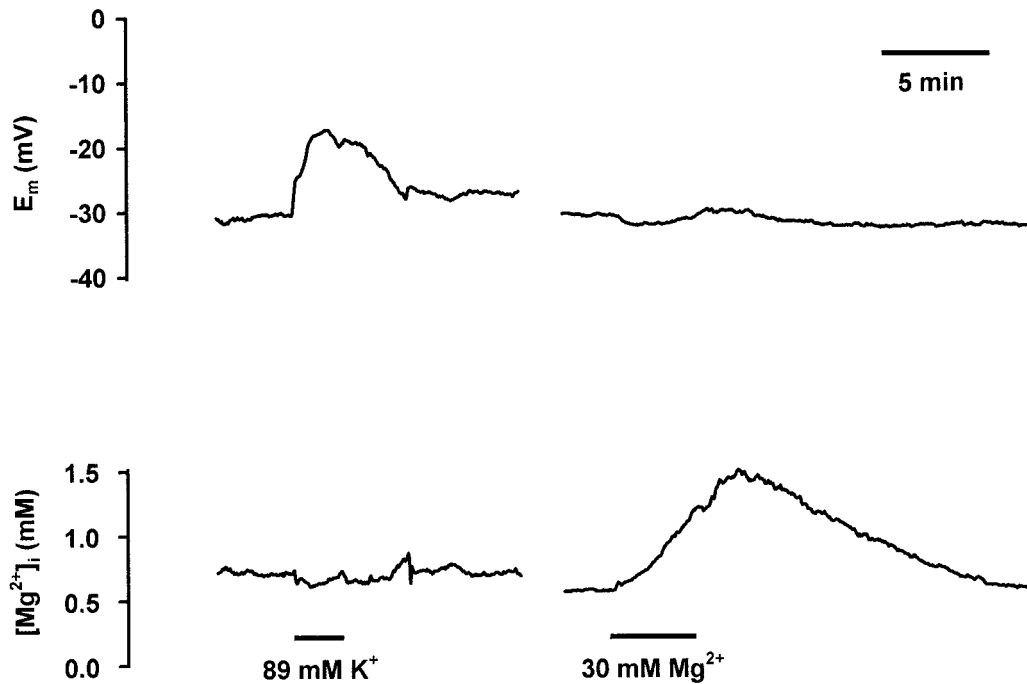


Figure 4. Recording of  $[Mg^{2+}]_i$  in a leech Retzius neurone with a  $Mg^{2+}$ -selective microelectrode based on ETH 5504. A  $Mg^{2+}$ -selective microelectrode based on ETH 5504 and a separate intracellular reference electrode were used to determine  $[Mg^{2+}]_i$  in a leech Retzius neurone. A depolarization of the neuronal membrane by increasing the extracellular  $K^+$ -concentration to 89 mM did not cause any changes in  $[Mg^{2+}]_i$ . Similar to the experiment shown in Figure 3, the neurone could be loaded with  $Mg^{2+}$  by increasing the extracellular  $Mg^{2+}$  concentration from 1 to 30 mM. The observed  $[Mg^{2+}]_i$  increase was fully reversible after decreasing the extracellular  $Mg^{2+}$  concentration back to 1 mM (gap: approx. 30 min).

recordings of  $[Mg^{2+}]_i$  could be combined with an iontophoretic injection of  $H^+$ ,  $OH^-$ , or  $Mg^{2+}$ .

#### ETH 7025, ETH 5506, ETH 5504

Compared to the  $Mg^{2+}$  sensors developed in the 80's, the newer sensors, namely ETH 7025 (Schaller *et al.* 1993), but especially ETH 5506 (O'Donnell *et al.* 1993, Spichiger and Fakler 1997) and ETH 5504 (X. Zhang *et al.* 1998) have excellent selectivities for  $Mg^{2+}$  over all major physiologically relevant ions. The reported selectivity data (X. Zhang *et al.* 1998) suggest that  $s_{physiol}$  of electrodes based on ETH 5504 should be  $> 90\%$  for  $[Mg^{2+}]_i$  values as low as 0.1 mM (Figure 2A). The selectivity for  $Mg^{2+}$  over  $Ca^{2+}$  should even be sufficient to allow determinations of the extracellular  $Mg^{2+}$  concentration, i.e., in the presence of millimolar  $Ca^{2+}$  concentrations. However, while these sensors have been successfully used for  $Mg^{2+}$  selective macroelectrodes (see below) their usefulness for microelectrodes has yet to be demonstrated. The fundamental difference between ETH 1117 / ETH 5214 and all newer sensors (ETH 7025, ETH 5506, ETH

5504) is the composition of the membrane matrix. While both ETH 1117 and ETH 5214 work in a true liquid membrane, ETH 7025 / ETH 5506 / ETH 5504 require the presence of PVC. To enable filling of a microelectrode, the PVC has to be dissolved, e.g., in THF or cyclohexanone. After filling, the evaporation of these substances causes the sensor column to shrink considerably. This eventually results in a tearing of the sensor column or a withdrawal of the column from the electrode tip. In both cases the microelectrodes will be non-functional. The risk for tearing of the sensor column can be reduced by minimizing the height of the sensor column. This, however, can only be achieved by front-filling the electrodes, which requires larger electrode tips and which, from our experience, makes the construction of double-barrelled microelectrodes impossible. Therefore, the use of these electrodes is limited to cells large enough to tolerate the impalement of two separate microelectrodes, such as frog oocytes and some large invertebrate neurones or muscle fibres.

To our knowledge there is, so far, no report on the successful use of microelectrodes based on ETH 7025 and ETH 5506. The only report of the successful use of microelectrodes based on ETH 5504 does not concern a determination of  $[Mg^{2+}]_i$  in a living cell but  $Mg^{2+}$  measurements in small (50  $\mu$ l) samples of rat serum (X. Zhang *et al.* 1998).

Our own, as yet preliminary, data for microelectrodes based on ETH 7025 and especially on ETH 5504 are very promising but also show that further adjustments are needed before these sensors can replace ETH 5214 in physiological experiments. Microelectrodes filled with ETH 7025 or ETH 5504 were both greatly superior to microelectrodes based on the sensor ETH 5214, as long as the tip size of the electrodes was in the range of about 5  $\mu$ m. In calibration solutions mimicking intracellular conditions (80 mM KCl, 10 mM NaCl, nominally  $Ca^{2+}$ -free, see Figure 2B), microelectrodes based on ETH 7025 had a maximum slope of  $-30.6 \pm 1.73$  mV/decade and a detection limit of  $39.0 \pm 7.6$   $\mu$ M ( $n = 3$ ). Microelectrodes based on ETH 5504 even had a mean detection limit of  $7.2 \pm 4.7$   $\mu$ M at a mean slope of  $-28.7 \pm 1.47$  mV/decade ( $n = 3$ , Figure 2B). As shown in Figure 1, this detection limit is actually low enough to allow the determination of the free  $Mg^{2+}$  concentration in a nominally  $Mg^{2+}$ -free solution.

If, however, the tip-size was reduced to below 1  $\mu$ m, to enable impalement into cells, the properties of the electrodes changed considerably. Initially, none of these microelectrodes showed any  $Mg^{2+}$ -sensitivity. Sensitivity could be partially restored by bevelling and we assume that the complete loss of sensitivity is mainly due to the formation of a dead space at the very tip of the electrode, due to the shrinking of the sensor column. After bevelling, the mean slope of electrodes based on ETH 7025 amounted to  $-27.5 \pm 1.9$  mV/decade while the detection limit increased to  $0.15 \pm 0.05$  mM ( $n = 4$ , Figure 2B). The detection limit thus was significantly higher than the detection limits found for electrodes based on ETH 5214. In contrast, bevelled microelectrodes based on ETH 5504 had a mean slope of  $-25.5 \pm 1.0$  mV/decade and a detection limit of  $45 \pm 23$   $\mu$ M ( $n = 3$ ), well below any microelectrode based on ETH 5214, but still significantly above ETH 5504 based microelectrodes with large tips (Figure 2B). It will now be the principal task to further improve the composition of the membrane matrix to minimize shrinking of the sensor column and to further reduce membrane resistance (Spichiger & Fakler

1997) to optimize the performance of these sensors in microelectrodes.

Some preliminary experiments with microelectrodes based on the sensor ETH 7025 in leech Retzius neurones resulted in a mean  $[Mg^{2+}]_i$  of 0.36 mM (pMg of  $3.45 \pm 0.12$ ) at a mean  $E_m$  value of  $-36.7 \pm 5.0$  mV ( $n = 3$ ) which was not significantly different from the values obtained with electrodes based on the sensor ETH 5214 ( $[Mg^{2+}]_i = 0.46$  mM, pMg =  $3.34 \pm 0.23$ ,  $E_m = 35.6 \pm 6.1$  mV,  $n = 32$ ). An example of an intracellular recording in a leech Retzius neurone using a microelectrode based on ETH 5504 is shown in Figure 4. The trace shows that  $[Mg^{2+}]_i$  is not affected by a depolarization of the cell in the presence of high (89 mM) extracellular  $K^+$  concentrations. Similar to the experiment shown in Figure 3B,  $[Mg^{2+}]_i$  increases during an increase in the extracellular  $Mg^{2+}$  concentration from 1 to 30 mM and returns to its original level upon the reduction of the extracellular  $Mg^{2+}$  concentration back to 1 mM. These results demonstrate that electrodes based on ETH 7025 and ETH 5504 are functional and can be applied to living cells.

### **$Mg^{2+}$ -selective macroelectrodes**

While the new, PVC-based  $Mg^{2+}$  sensors still have to be optimized for their general application in microelectrodes for the determination of  $[Mg^{2+}]_i$ , they have been very successfully used in macroelectrodes. Both ETH 7025 (Zhang *et al.* 1995) and ETH 5506 (Lüthi *et al.* 1997) were used for the construction of macroelectrodes that are less than 5 mm in diameter and thus enable measurements in very small volumes. Electrodes based on ETH 5506 can reliably be calibrated down to 1  $\mu$ M (Lüthi *et al.* 1997).

Although these electrodes are far too large to be used for a direct determination of  $[Mg^{2+}]_i$  they can nonetheless provide information on possible changes in  $[Mg^{2+}]_i$ , e.g. from measurements in cell-lysates. Thus, an estimate of  $[Mg^{2+}]_i$  could be obtained for young and mature spinach chloroplasts, showing, that  $[Mg^{2+}]_i$  rises more than twofold during chloroplast maturation (Horlitz & Klaff, 2000). This study supports the hypothesis that  $Mg^{2+}$  may be the physiological regulator of the differential mRNA stability observed during leaf maturation.

Furthermore, these electrodes have been used for a direct determination of the intracellular  $Mg^{2+}$  buffering either by titrating cell lysates (Günther *et al.*

1995) or by the determination of the  $Mg^{2+}$  binding properties of substances such as ATP (Zhang *et al.* 1997; Lüthi *et al.* 1999) which is considered a major intracellular  $Mg^{2+}$  buffer.

The ionophore ETH 7025 is also routinely used in commercially available equipment for the determination of  $[Mg^{2+}]$  in blood samples (Marsoner *et al.* 1994).

## Conclusions

The development of sensors for the measurement of  $Mg^{2+}$  over the past two decades and especially during the past few years has been very successful. The greatest achievement is that ETH 5506 and 5504, which are truly  $Mg^{2+}$ -selective sensors, allow  $Mg^{2+}$ -determinations in an extracellular environment, i.e. in the presence of millimolar  $Ca^{2+}$  concentrations.  $Mg^{2+}$ -selective microelectrodes have not yet profited from the new sensors, as the membrane compositions have not yet been optimized. Preliminary experiments, however, look very promising. The greatest drawback of the new generation of  $Mg^{2+}$ -sensors is their requirement of the PVC in the membrane matrix which complicates the construction of functional microelectrodes.

## Acknowledgements

We would like to thank S. Durry for expert technical assistance and Prof. J.A.S. McGuigan for critically reading the manuscript. ETH 5504 was a generous gift from the Centre for Chemical Sensors, ETH Zürich, Switzerland (A. Fakler and Prof. U.E. Spichiger).

## References

- Ammann D. 1986 Ion-Selective Microelectrodes. Principles, Design and Application. Berlin: Springer Verlag.
- Alvarez-Leefmans FJ, Gamiño SM, Rink TJ. 1984 Intracellular free magnesium in neurones of *Helix aspersa* measured with ion-selective micro-electrodes. *J Physiol (Lond)* **354**, 303–317.
- Alvarez-Leefmans FJ, Gamiño SM, Giraldez F, González-Serratos H. 1986 Intracellular free magnesium in frog skeletal muscle fibres measured with ion-selective micro-electrodes. *J Physiol (Lond)* **378**, 461–483.
- Alvarez-Leefmans FJ, Giraldez F, Gamiño SM 1987 Intracellular free magnesium in excitable cells: its measurement and its biologic significance. *Can J Physiol Pharmacol* **65**, 915–925.
- Blatter LA, McGuigan JAS. 1986 Free intracellular magnesium concentration in ferret ventricular muscle measured with ion selective micro-electrodes. *Quart J Exp Physiol* **71**, 467–473.
- Blatter LA, McGuigan JAS. 1988 Estimation of the upper limit of the free magnesium concentration measured with  $Mg$ -sensitive microelectrodes in ferret ventricular muscle: (1) use of the Nicolsky-Eisenman Equation and (2) in calibration solutions of the appropriate concentration. *Magnesium* **7**, 154–165.
- Borrelli MJ, Carlini WG, Dewey WC, Ransom BR. 1985 A simple method for making ion-selective microelectrodes suitable for intracellular recording in vertebrate cells. *J Neurosci. Meth.* **15**, 141–154.
- Buri A, Chen S, Fry CH, Illner H, Kickenweiz E, McGuigan JAS, Noble D, Powell T, Twist VW. 1993 The regulation of intracellular  $Mg^{2+}$  in guinea-pig heart, studied with  $Mg^{2+}$ -selective microelectrodes and fluorochromes. *Exp Physiol* **78**, 221–233.
- Buri A, McGuigan JAS. 1990 Intracellular free magnesium and its regulation, studied in isolated ferret ventricular muscle with ion-selective microelectrodes. *Exp Physiol* **75**, 751–761.
- Caldwell PC. 1954 An investigation of the intracellular pH of crab muscle fibres by means of micro-glass and micro-tungsten electrodes. *J Physiol (Lond)* **126**, 169–180.
- Coles JA, Tsacopoulos M. 1977 A method of making fine double-barrelled potassium-sensitive micro-electrodes for intracellular recording. *J Physiol (Lond)* **270**, 13–14P.
- Gasser RNA. 1990 A microelectrode study of the mechanisms of ionic and electrical changes during simulated ischaemia in isolated cardiac muscle. D. Phil. Thesis, Oxford.
- Günther T, Vormann J, McGuigan JAS. 1995 Buffering and activity coefficient of intracellular free magnesium concentration in human erythrocytes. *Biochem. Molec. Biol. Int.* **37**, 871–875.
- Günzel D, Galler S. 1991 Intracellular free  $Mg^{2+}$  concentration in skeletal muscle fibres of frog and crayfish. *Pflügers Arch* **417**, 446–453.
- Günzel D, Schlue W-R. 1996 Sodium / magnesium antiport in Retzius neurones of the leech *Hirudo medicinalis*. *J Physiol (Lond)* **491**, 595–608.
- Günzel D, Schlue W-R. 1997 Interactions between magnesium, sodium and intracellular pH in leech Retzius neurones. In: Smetana R., ed. *Advances in Magnesium Research*. London: John Libbey; 497–506.
- Günzel D, Schlue W-R. 2000 Mechanisms of  $Mg^{2+}$  influx, efflux and intracellular 'muffling' in leech neurones and glial cells. *Magn Res.* **13**, 123–138.
- Günzel D, Durry S, Schlue W-R. 1997 Intracellular alkalization causes  $Mg^{2+}$  release from intracellular binding sites in leech Retzius neurones. *Pflügers Arch* **435**, 65–73.
- Günzel D, Müller A, Durry S, Schlue W-R. 1999 Multi-barrelled ion-sensitive microelectrodes and their application in microdroplets and biological systems. *Electrochim. Acta* **44**, 3785–3793.
- Günzel D, Zimmermann F, Durry S, Schlue W-R. 2001 Apparent intracellular  $Mg^{2+}$  buffering in neurones of the leech *Hirudo medicinalis*. *Biophys J* **80**, 1298–1310.
- Fry CH, Hall SK, Blatter LA, McGuigan JAS. 1990 Analysis and presentation of intracellular measurements obtained with ion-selective microelectrodes. *Exp Physiol* **75**, 187–198.
- Hess P, Metzger P, Weingart R. 1982 Free magnesium in sheep, ferret and frog striated muscle at rest measured with ion-selective micro-electrodes. *J Physiol (Lond)* **333**, 173–188.
- Hintz K, Günzel D, Schlue W-R. 1999  $Na^{+}$ -dependent regulation of the free  $Mg^{2+}$  concentration in neuropile glial cells and P neurones of the leech *Hirudo medicinalis*. *Pflügers Arch* **437**, 345–362.
- Horlitz M, Klaff P. 2000 Gene-specific *trans*-regulatory functions of magnesium for chloroplast mRNA stability in higher plants. *J Biol Chem* **275**, 35638–35645.

- Hu Z, Bühner T, Müller M, Rusterholz B, Rouilly M, Simon W. 1989 Intracellular magnesium ion selective microelectrode based on a neutral carrier. *Anal Chem* **61**, 574–576.
- Kennedy HJ. 1998 Intracellular  $Mg^{2+}$  regulation in voltage-clamped *Helix aspersa* neurones measured with mag-fura-2 and  $Mg^{2+}$ -sensitive microelectrodes. *Exp Physiol* **83**, 449–460.
- Lanter F, Erne D, Ammann D, Simon W. 1980 Neutral carrier based ion-selective electrode for intracellular magnesium activity studies. *Anal Chem* **52**, 2400–2402.
- Lopez JR, Alamo L, Caputo C, Vergara J, DiPolo R. 1984 Direct measurement of intracellular free magnesium in frog skeletal muscle using magnesium-selective microelectrodes. *Biochim Biophys Acta* **804**, 1–7.
- Lüthi D, Spichiger U, Forster I, McGuigan JAS. 1997 Calibration of  $Mg^{2+}$ -selective macroelectrodes down to  $1 \mu\text{mol l}^{-1}$  in intracellular and  $Ca^{2+}$ -containing extracellular solutions. *Exp Physiol* **82**, 453–467.
- Lüthi D, Günzel D, McGuigan JAS. 1999  $Mg$ -ATP binding: its modification by spermine, the relevance to cytosolic  $Mg^{2+}$  buffering, changes in the intracellular ionized  $Mg^{2+}$  concentration and the estimation of  $Mg^{2+}$  by  $^{31}\text{P}$ -NMR. *Exp Physiol* **84**, 231–252.
- MacDermott M. 1990 The intracellular concentration of free magnesium in extensor digitorum longus muscles of the rat. *Exp Physiol* **75**, 763–769.
- Marsoner HJ, Spichiger UE, Ritter C, Sachs C, Ghahramani M, Offenbacher H, Kroneis H, Kindermans C, Dechaux M. 1994 Measurement of ionized magnesium with neutral carrier based ISE's. Progress and results with the AVL 988-4 magnesium analyzer. *Scand J Clin Lab Invest* **54** (Suppl. 217), 45–51.
- McGuigan JAS, Blatter LA. 1989 Measurement of free magnesium using magnesium selective microelectrodes. *Magnesium-Bull.* **11**, 139–142.
- McGuigan JAS, Blatter LA, Buri A. 1990 Use of ion selective microelectrodes to measure intracellular free  $Mg^{2+}$ . In: Strada P, Carbone E, ed.  *$Mg^{2+}$  and Excitable Membranes*. Berlin: Springer-Verlag.
- McGuigan JAS, Buri A, Chen S, Illner H, Lüthi D. 1993 Some theoretical and practical aspects of the measurement of the intracellular free magnesium concentration in heart muscle: Consideration of its regulation and modulation. In: Birch NJ, ed. *Magnesium and the Cell*. London: Academic Press.
- Mooren FC, Turi S, Günzel D, Schlue W-R, Domschke W, Singh J, Lerch MM. 2001 Calcium - magnesium interactions in pancreatic acinar cells. *FASEB J.* **15**, 659–672.
- Müller A, Günzel D, Schlue W-R. 1997a Stoichiometry of sodium/magnesium antiport in leech Retzius neurones. In: Smetana R, *Advances in Magnesium Research*. London: John Libbey; 507–513.
- Müller A, Günzel D, Schlue W-R. 1997b Effect of kainate on  $[Mg^{2+}]_i$ ,  $[Na^+]_i$ ,  $pH_i$  and  $E_m$  in leech Retzius neurones. *Magnesium-Bull* **19**, 128.
- Munoz J-L, Deyhimi F, Coles JA. 1983 Silanization of glass in the making of ion-sensitive microelectrodes. *J Neurosci Meth* **8**, 231–247.
- Munsch T, Reinhard C, Deitmer JW. 1995 Die intrazelluläre Magnesium-Konzentration identifizierter Neurone und Gliazellen aus dem Zentralnervensystem des Blutegels. *Proc German Zool Soc* **88**, 11.
- O'Donell J, Li HB, Rusterholz B, Pedrazza U, Simon W. 1993 Development of magnesium-selective ionophores. *Anal Chim Acta* **281**, 129–134.
- Orme FW. 1969 Liquid ion-exchanger microelectrodes. In: Lavallée M, Schanne OF, Hebert NC, eds. *Glass Microelectrodes*. New York: John Wiley & Sons, Inc.
- Rönnau K. 1984 A simplified method for silanization of doublebarrelled ion-sensitive microelectrodes. *Experientia* **40**, 1019–1020.
- Schaller U, Spichiger UE, Simon W. 1993 Novel magnesium ion-selective microelectrodes based on a neutral carrier. *Pflügers Arch* **423**, 338–342.
- Spichiger UE, Fakler A. 1997 Potentiometric microelectrodes as sensors and detectors. Magnesium-selective electrodes as sensors, and Hofmeister electrodes as detectors for histamine in capillary electrophoresis. *Electrochim Acta* **42**, 3137–3145.
- Thomas RC. 1978 *Ion-Sensitive Intracellular Microelectrodes. How to Make and Use Them*. London: Academic Press.
- Tsien RY, Rink TJ. 1981 Neutral carrier ion-selective microelectrodes for measurement of intracellular free calcium. *Biochim Biophys Acta* **599**, 623–638.
- Walker JL. 1971 Ion specific liquid ion exchanger microelectrodes. *Anal Chem* **43**(3), 89A–92A.
- Zhang W, Truttmann AC, Lüthi D, McGuigan JAS. 1995 The manufacture and characteristics of magnesium selective macroelectrodes. *Magnesium-Bull.* **17**, 125–130.
- Zhang W, Truttmann AC, Lüthi D, McGuigan JAS. 1997 Apparent  $Mg^{2+}$ -adenosine 5-triphosphate dissociation constant measured with  $Mg^{2+}$  macroelectrodes under conditions pertinent to  $^{31}\text{P}$  NMR ionized magnesium determinations. *Anal Biochem* **251**, 246–250.
- Zhang W, Fakler A, Demuth C, Spichiger UE. 1998 Comparison of different methods for determining the selectivity coefficient using a magnesium-selective electrode. *Anal Chim Acta* **375**, 211–222.
- Zhang X, Fakler A, Spichiger UE. 1998 Development of magnesium-ion-selective microelectrodes based on a new neutral carrier ETH<sup>T</sup> 5504. *Electroanalysis* **10**, 1174–1181.